Weak Response of Metallic Single-Walled Carbon Nanotubes to C60 Encapsulation Studied by Resonance Raman Spectroscopy

ARTICLE *in* THE JOURNAL OF PHYSICAL CHEMISTRY C · OCTOBER 2012

Impact Factor: 4.77 · DOI: 10.1021/jp309379r

4 AUTHORS:

Soon-Kil Joung
FOOSUNG Co. Ltd
16 PUBLICATIONS **399** CITATIONS
SEE PROFILE

Toshiya Okazaki
National Institute of Advanced Industrial Scie…
136 PUBLICATIONS **4,207** CITATIONS
SEE PROFILE

Susumu Okada
University of Tsukuba
221 PUBLICATIONS **3,333** CITATIONS
SEE PROFILE

Sumio Iijima
Meijo University
599 PUBLICATIONS **32,661** CITATIONS
SEE PROFILE

THE JOURNAL OF PHYSICAL CHEMISTRY C

Article

pubs.acs.org/JPCC

Weak Response of Metallic Single-Walled Carbon Nanotubes to C_{60} Encapsulation Studied by Resonance Raman Spectroscopy

Soon-Kil Joung,[†,‡] Toshiya Okazaki,*[,†,‡] Susumu Okada,[§,∥] and Sumio Iijima[†,‡]

[†]National Institute of Advanced Industrial Science and Technology (AIST), Tsukuba 305-8565, Japan

[‡]Technology Research Association for Single Wall Carbon Nanotubes (TASC), c/o Nanotube Research Center, AIST, Tsukuba 305-8565, Japan

[§]Institute of Physics and Center for Computational Sciences, University of Tsukuba, 1-1-1 Tennodai, Tsukuba 305-8577, Japan

[∥]CREST, Japan Science and Technology Agency (JST), 4-1-8 Honcho, Kawaguchi 332-0012, Japan

Supporting Information

ABSTRACT: Metallic single-walled carbon nanotubes (SWCNTs) have been regarded as unique quasi-1D metallic systems. Their basic properties significantly differ from those of their semiconducting counterparts even though their chemical compositions and sizes are nearly identical to each other. In this study, we investigate the effects of C_{60} fullerene encapsulation on the phonon and electronic properties of metallic SWCNTs by resonance Raman spectroscopy. The changes in the radial breathing mode frequencies and the optical transition energies after C_{60} insertions show characteristic tube diameter dependences, as in the case of the corresponding semiconducting SWCNTs. Although the observed behaviors can be attributed to the intermolecular interaction between SWCNTs and the encapsulated C_{60}, similar to the corresponding semiconducting SWCNTs, the strength of the interaction is measurably weaker than that of semiconducting SWCNTs. The present findings provide important insight into the essential differences in the basic nature of metallic and semiconducting SWCNTs.

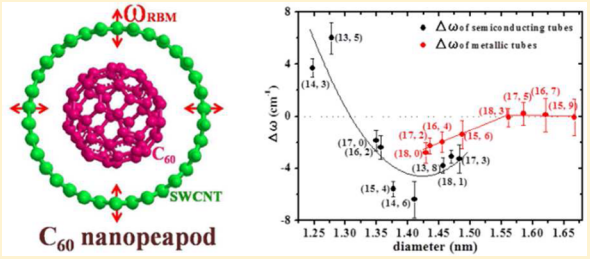

INTRODUCTION

One of the remarkable properties of single-walled carbon nanotubes (SWCNTs) is that they show metallic or semiconducting properties depending on the tube diameter and the wrapping angle.[1,2] In particular, metallic SWCNTs can be regarded as unique metallic materials because the free electrons in SWCNTs are confined to 1D channels in contrast with those in bulk metals. In such 1D wires, increased interaction causes electrons to behave in a highly cooperative way, and the Fermi liquid theory no longer applies in such cases.[3] Indeed, strongly correlated electron behaviors such as the Tomonaga−Luttinger liquid state and the Mott insulating state have been observed in experiments on metallic SWCNTs.[4,5]

For SWCNTs to be used in practical applications such as transparent electrodes,[6,7] the separation of metallic SWCNTs from their semiconducting counterparts is a highly important process. Recently, several effective methods have been developed to separate metallic and semiconducting SWCNTs.[8−13] These methods generally utilize the electronic-structure-dependent differences in the interactions between SWCNTs and the adsorbed molecules. For example, fluorene-based polymers such as poly(9,9-di-*n*-octylfluorene) (PFO) dissolve semiconducting SWCNTs with specific chiral indices in organic solvents.[10,11,13] In such polymer-wrapping extraction, only the semiconducting SWCNTs can be extracted, probably because of the stronger interaction between the polymer and semiconducting SWCNTs than that between the polymer and the metallic counterparts. In the agarose gel method,[12] semiconducting SWCNTs are selectively attached to agarose gel beads in a column, and the eluent that contains only metallic SWCNTs emerges first. Subsequently, the remaining semiconducting SWCNTs are collected by adding further solvents. These elution behaviors indicate that the interaction between the semiconducting SWCNTs and the gel may be stronger than that between metallic SWCNTs and the gel. Although the observed experimental results have usually been explained by the difference in the interaction between metallic and semiconducting SWCNTs, the details still remain unclear. Thus, the investigation of the difference in the intermolecular interaction between metallic and semiconducting SWCNTs is still essential to understand the fundamental nature of SWCNTs.

SWCNTs encapsulating fullerenes, the so-called nanopeapods (NPDs), can be regarded as model material for investigating the intermolecular interaction between SWCNTs and organic molecules.[14−20] Because the distance between SWCNTs and the encapsulated molecules can be varied on the angstrom scale, precise and systematic investigations are possible.[21−23] Photoluminescence (PL) and Raman studies have

Received: September 21, 2012
Revised: October 21, 2012
Published: October 22, 2012

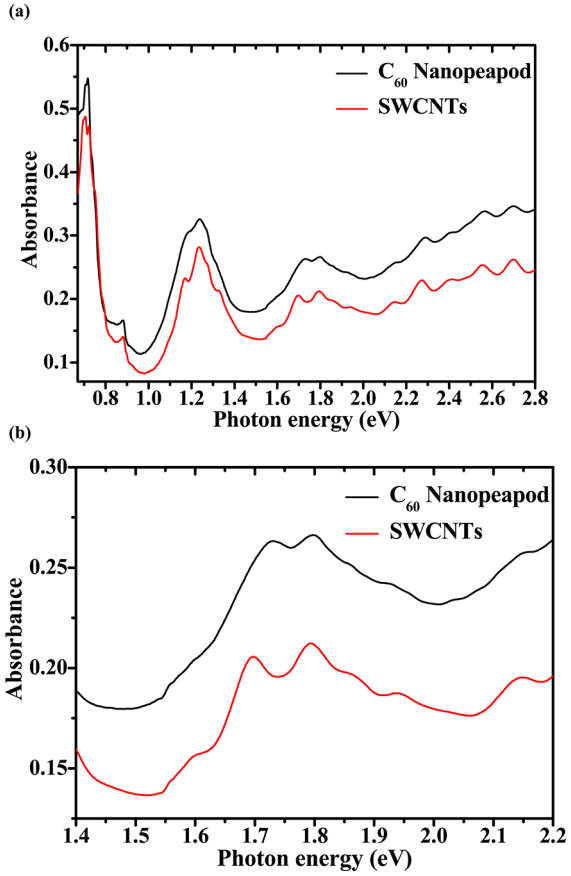

Figure 1. (a) Optical absorption spectra of C_{60} nanopeapods (NPDs) and original SWCNTs in SDBS-D_2O solutions. (b) Expanded absorption spectra in the E^M_{11} region.

revealed that the interaction between semiconducting SWCNTs and encapsulated fullerenes such as C_{60},[24−27] C_{70},[28] and azafullerenes[29] can be explained by the van der Waals-type intermolecular interaction; such interaction is very sensitive to the interspacing between SWCNTs and the fullerenes. Even though there have been many reports on the effects of fullerene encapsulation on the electronic properties of SWCNTs,[30−33] the difference in the response between semiconducting and metallic SWCNTs has still not been properly examined.

For monitoring the interaction between metallic SWCNTs and the encapsulated molecules, Raman spectroscopy is one of the most suitable and efficient techniques because metallic SWCNTs do not exhibit PL.[26,27,34] The radial breathing mode (RBM) phonon of SWCNTs is particularly useful because its frequency is directly related to the inverse tube diameter $(1/d_t)$, and this frequency is sensitive to molecular encapsulation. Because of the resonance effect, the Raman intensity of SWCNTs drastically changes with the molecular structure and the excitation wavelength. Although the shift in the RBM frequencies due to chemical and electrochemical doping has been frequently reported, the observed shifts appear to reflect the change in resonance enhancement in a mixture of SWCNTs rather than an actual shift in the RBM mode of a particular (n, m) tube.[34] Therefore, for comprehensive characterizations, it is necessary to measure the Raman spectra by using several laser excitation lines.

In this study, we report the effects of C_{60} fullerene encapsulation on the RBM frequencies and the optical transition energies of metallic SWCNTs by using resonance Raman spectroscopy with laser excitations tuned from 1.19 to 1.65 eV; these excitations correspond to the first optical transitions (E^M_{11}) in metallic SWCNTs with diameters of 1.3 to 1.5 nm. To study the above-mentioned effects, we constructed 2D contour maps of the resonance Raman intensities using C_{60} NPDs and an SWCNT control sample in a

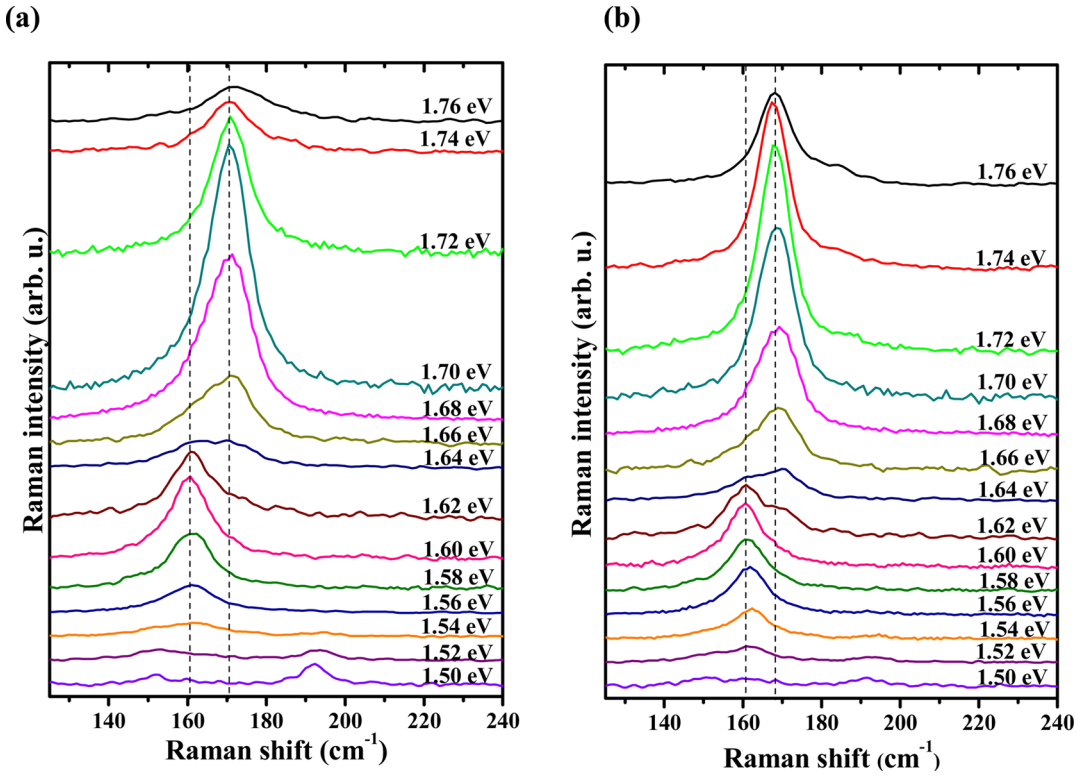

Figure 2. Resonance Raman spectra in RBM region of (a) original SWCNTs in SDBS-D_2O solution and (b) C_{60} NPDs in SDBS-D_2O solution under different excitation energies.

dx.doi.org/10.1021/jp309379r | J. Phys. Chem. C 2012, 116, 23844−23850

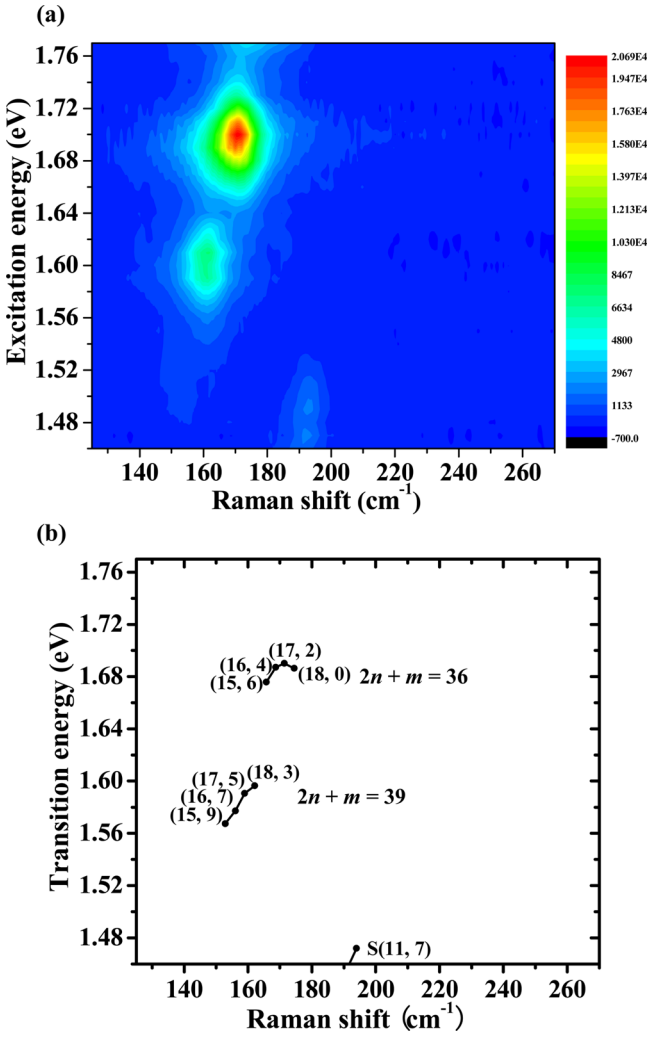

Figure 3. (a) 2D Raman intensity maps of RBM phonon regions of original SWCNTs. (b) RBM peak positions obtained by curve fitting analyses.

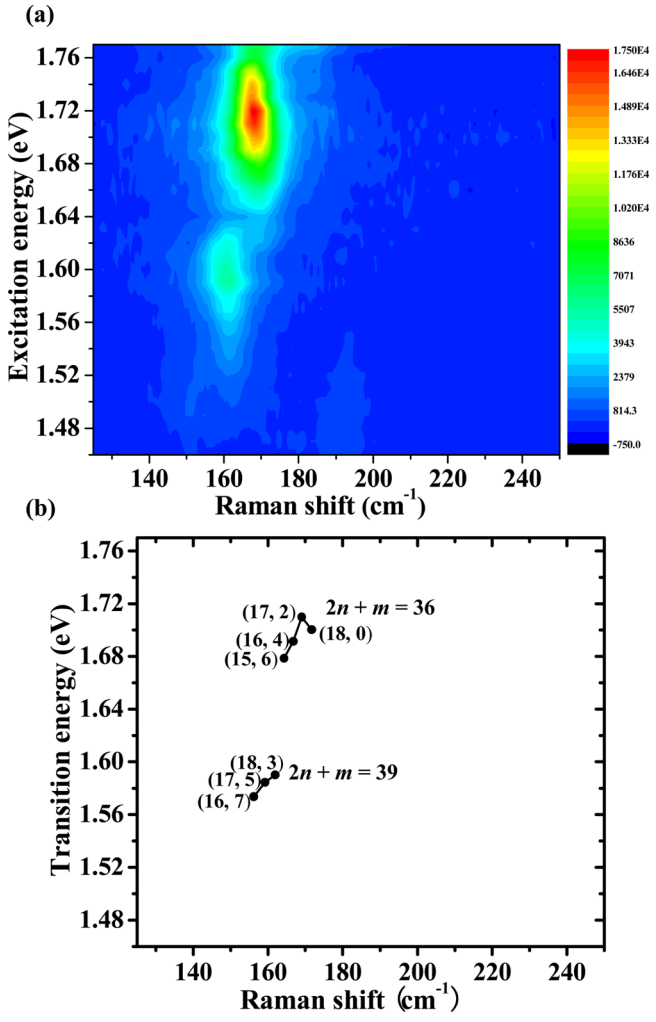

Figure 4. (a) 2D Raman intensity maps of RBM phonon regions of C_{60} NPDs in SDBS-D_2O. (b) RBM peak positions obtained by curve fitting analyses.

micelle solution. Although the observed frequency shifts in the RBM phonon and the change in the optical transition energies are reasonably explained by the intermolecular interaction between metallic SWCNTs and the encapsulated C_{60} (as is the case for semiconducting NPDs),[24−27] the estimated strength of the interaction is considerably smaller, thereby suggesting weaker interaction of metallic SWCNTs than semiconducting SWCNTs with the encapsulated C_{60}.

EXPERIMENTAL SECTION

The details of the C_{60} NPD synthesis have been previously reported.[25] In brief, purified SWCNTs (Meijo Arc APJ-type, Meijo Nano Carbon) were heated at 570 °C for 30 min in air to open the end caps. The treated SWCNTs and C_{60} were sealed under vacuum (~10^{-4} Pa) in quartz tubes and heated to 600 °C for 96 h. The obtained NPDs were washed with toluene to remove the fullerenes adsorbed on the outside of the walls. For the Raman measurements, SWCNTs and NPD samples were dispersed in D_2O with 1 wt % sodium dodecylbenzene sulfonate (SDBS) by using a tip-type sonicator (Sonics VCX500, operated at 200 W for 10 min) and subsequently centrifuged at 127 600*g* for 2.5 h. After centrifugation, the supernatant was collected for the measurements.

Optical absorption spectra were recorded with a Hitachi U-4100 spectrometer. Resonance Raman spectroscopy was performed with a triple-grating monochromator (Bunko-Keiki BRM-900) equipped with an InGaAs diode array (Princeton Instruments OMA-V1.7). A tunable Ti-sapphire laser (Spectra Physics 3900S) was used as the excitation source. We normalized the Raman intensity with respect to the nonresonant Raman signal of chloroform.

RESULTS AND DISCUSSION

Figure 1a shows the UV−vis-NIR absorption spectrum of C_{60} NPDs in SDBS micelle solution, together with the reference spectrum of the unfilled SWCNTs. The first band-gap transition of metallic SWCNTs (E^{M}_{11}) with d_t = 1.25 to 1.55 nm is clearly observed in the range of 1.6 to 2.0 eV (Figure 1b). Subsequent to the C_{60} encapsulations, the absorption peak at 1.69 eV is shifted to 1.73 eV, which is consistent with the results of the RBM intensity map (see below). The peaks observed in the ranges of 0.6 to 1.0 eV and 1.0 to 1.5 eV correspond to the first (E^{S}_{11}) and the second (E^{S}_{22}) optical transitions in semiconducting SWCNTs, respectively.

Figure 2 shows the resonance Raman spectra of the original SWCNTs and C_{60} NPDs in the RBM frequency region under different excitation energies. In the spectra of the original SWCNTs (Figure 2a), prominent RBM phonon peaks are

dx.doi.org/10.1021/jp309379r | J. Phys. Chem. C 2012, 116, 23844−23850

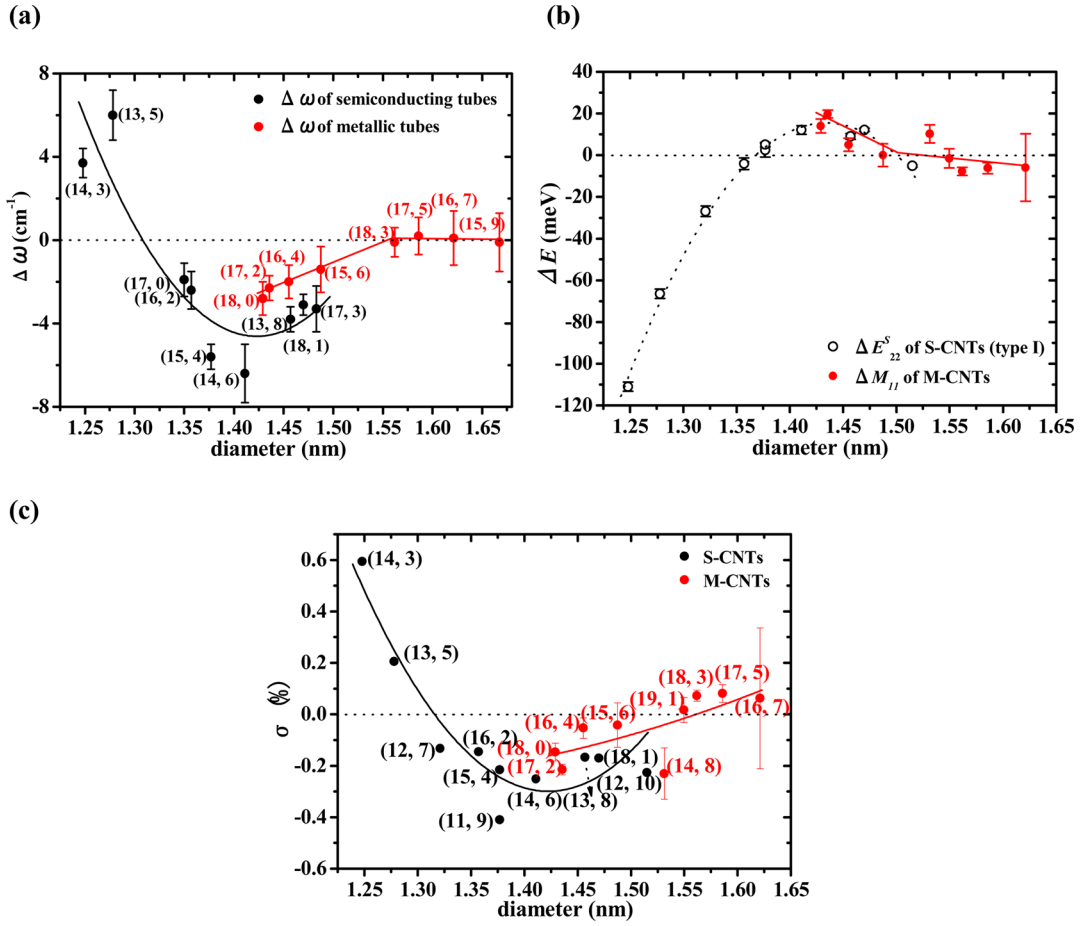

Figure 5. (a) Experimentally obtained $\Delta\omega$ (solid circles) for metallic C_{60} NPDs (red circles) and semiconducting C_{60} NPDs (black circles). (b) Optical transition energy shifts ($\Delta E = E^{M}_{11}$(NPDs) − E^{M}_{11}(SWCNTs)) as a function of tube diameter (red circles), together with reference data of type II semiconducting NPDs ($\Delta E = E^{S}_{11}$ (NPDs) − E^{S}_{11}(SWCNTs)) that are obtained by PL measurements.[24,25] (c) Values of σ calculated from ΔE.

observed at around 160 and 170 cm^{-1} under excitations of ~1.60 and ~1.70 eV, respectively, which corresponds to SWCNTs with diameters of 1.3 to 1.5 nm. These excitation peaks are consistent with the peaks in the absorption spectrum (Figure 1b). In the case of the C_{60} NPDs (Figure 2b), the spectral shapes and peak positions are very similar to those of the original SWCNTs (Figure 2a), whereas significant differences can be observed in the spectral shapes and peak positions of semiconducting NPDs.[26,27]

To assign these RBM phonon peaks to the respective (n, m) tubes, we constructed a 2D contour map from the resonance Raman spectra of the RBM phonon region from 1.50 to 1.76 eV. Figure 3a shows the 2D RBM intensity map of the SWCNT sample in the SDBS-D_2O solutions. The solid circles in Figure 3b indicate the RBM phonon peak positions in the individual (n, m) tubes obtained by line-shape fitting. (See the Supporting Information for details.) It is noteworthy that all of the RBM peaks can be reasonably assigned to each (n, m) C_{60} NPD. It was unnecessary to assume that the additional RBM peaks originated from another species. The obtained RBM phonon frequencies (ω_{RBM}) of the C_{60} NPDs and the corresponding SWCNTs are summarized in Supporting Information.

Typical $2n + m$ family patterns[35−37] are clearly observed in Figure 3b. The RBM phonon peaks appearing in the range of 150−170 cm^{-1} under the excitation wavelength region of 1.56 tp 1.60 eV belong to a single $2n + m$ branch. Another branch is clearly delineated in the frequency range of 170−180 cm^{-1} under excitation wavelengths from 1.67 to 1.69 eV. On the basis of the Raman results reported in a previous study,[35−37] the $2n + m$ branches observed in our results can be assigned to the $2n + m$ = 39 and 36 families, as shown in Figure 3b.

The 2D RBM intensity map of C_{60} NPDs is shown in Figure 4a. The general features are very similar to those of the SWCNT control sample (Figure 3a). The curve fitting analyses show the RBM peak positions in the map as depicted in Figure 4b. Although the peak positions of some RBMs are shifted, these peaks still show the typical "hooked" family pattern. Therefore, it is highly reasonable to assign the observed RBM peaks of C_{60} NPDs to each (n, m) tube after accounting for the "empty" SWCNTs, as denoted in Figure 4b. The obtained optical transition energies (E^{M}_{11}) of the C_{60} NPDs and the corresponding SWCNTs are summarized in Table S1 (Supporting Information).

To study the C_{60} encapsulation effect on the phonon and the electronic properties in further detail, we investigated the differences in the RBM frequency and the optical transition energies before and after insertion (Figure 5). Figure 5a shows the RBM frequency shifts ($\Delta\omega = \omega_{RBM}$ (NPDs) − ω_{RBM} (SWCNT)) as a function of the tube diameter (red circles), together with the reported data of the semiconducting NPDs.[26,27]

In the case of the semiconducting NPDs, we found that the upshifts ($\Delta\omega > 0$) for d_t < ~1.3 nm and the downshifts ($\Delta\omega < 0$) for d_t < ~1.3 nm result from the repulsive and the attractive

dx.doi.org/10.1021/jp309379r | J. Phys. Chem. C 2012, 116, 23844−23850

interactions, respectively, between SWCNTs and the encapsulated C_{60}.[26,27] For instance, in the smaller diameter regime (d_t < 1.3 nm), the small interspacing between the tube wall and the C_{60} cage induces steric hindrance of the radial motion of SWCNTs, thereby resulting in the upshift of the RBM frequency.[26,27] With increasing interspacing (d_t > ~1.3 nm), the attractive intermolecular interaction becomes dominant, and this results in the downward shift of RBM phonon frequencies.[26,27] Interestingly, the smallest value of $\Delta\omega$ (= −6 cm^{-1}) was observed at an interspacing of ~0.35 nm (d_t = 1.41 nm); this distance is similar to the interlayer distance for graphite (0.335 nm).[38] Naturally, the interaction between the SWCNTs and the encapsulated C_{60} becomes weaker as the distance between the tube wall and C_{60} increases. Consequently, the RBM frequency difference approaches zero ($\Delta\omega$ = 0).

The observed downshifts ($\Delta\omega$ < 0) for metallic NPDs in the larger diameter region can be explained by the same mechanism (Figure 5a). In fact, the effective interaction between the π states of the metallic SWCNTs and C_{60} has been predicted using theoretical calculations.[39] The subsequent expansion of the π-electron cloud of SWCNTs and C_{60} decreases the force constant of the C−C bond, thereby leading to the downward shift of RBM phonon frequencies after C_{60} encapsulation.[39]

Although the diameter dependence of $\Delta\omega$ of metallic NPDs is consistent with that of semiconducting NPDs, the amount of the frequency shifts is about half of that for the semiconducting NPDs. A simple explanation for the smaller frequency shifts is that the interaction between metallic SWCNTs and C_{60} is weaker than that between semiconducting SWCNTs and C_{60}.

It is well-known that the RBM frequency of metallic SWCNTs is downshifted due to strong electron−phonon (*e*-ph) coupling.[40,41] In fact, an upshift of the RBM frequency was observed when the Fermi energy level was changed by electrochemical doping.[40,41] To check whether the strength of the electron−phonon coupling changes upon C_{60} encapsulations, we measured the G-mode of the NPDs and the original SWCNTs because the tangential G-mode is very sensitive to the *e*-ph interaction.[40] In particular, the peak positions and the line width of the longitudinal optical (LO) G^--band severely decrease upon doping.[40] Under the excitation energies of 1.60 and 1.70 eV, we observed typical G-mode signals corresponding to metallic SWCNTs (Figure 6). The spectral shape of the G-mode does not change after C_{60} encapsulation. In particular, the peak positions and the line width of G^--bands at around 1560−1570 cm^{-1} do not show significant change. Hence, the strength of the *e*-ph coupling should be similar for both SWCNTs and NPDs, and it may be reasonable to neglect the *e*-ph effects on the RBM shifts observed in our experiment.

The optical transition energy shifts ($\Delta E = E^M_{11}$(NPDs) − E^M_{11}(SWCNTs)) are also plotted as a function of tube diameter (red circles), together with reference data of type II semiconducting NPDs ($\Delta E = E^S_{11}$(NPDs) − E^S_{11}(SWCNTs)) that are obtained by the PL measurements (open circles) (Figure 5b).[24,25] It appears that ΔE for metallic NPDs almost overlaps with that for type II semiconducting NPDs.

For type II semiconducting NPDs, it has been found that the red shifts (ΔE < 0) for d_t < ~1.35 nm and the blue shifts (ΔE > 0) for d_t > ~1.35 nm can also be explained by the van der Waals-type intermolecular interaction between C_{60} and SWCNTs.[24−27] A quantitative similarity of the blue shifts of metallic NPDs suggests that the observed shifts are induced by the attractive forces between metallic SWCNTs and C_{60}. In particular, an increase in attractive interaction can be interpreted as an effect similar to that caused by

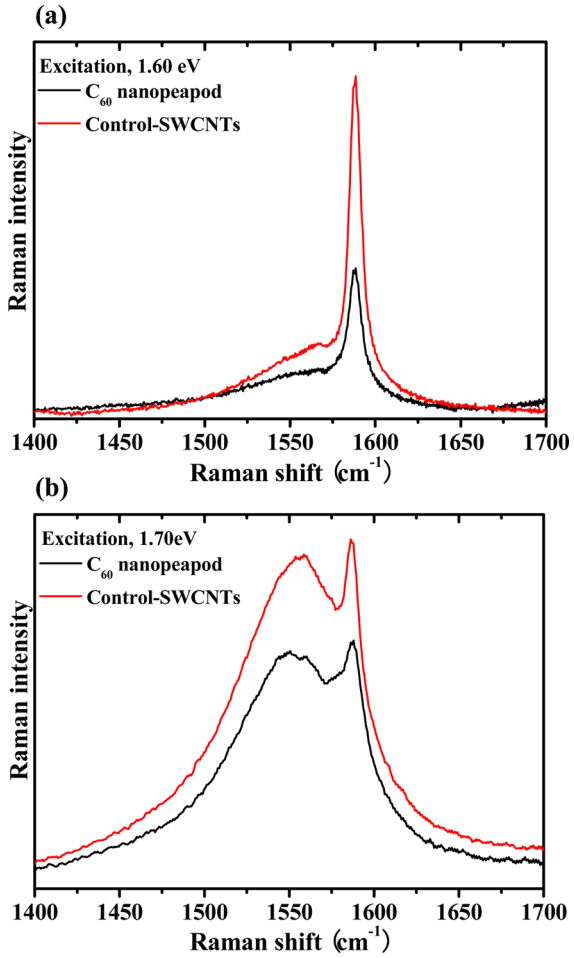

Figure 6. Resonance Raman spectra in the G-band region of C60 NPDs and SWCNTs at excitation energies of (a) 1.60 and (b) 1.70 eV.

reduction in the effective tube diameter.[24,25] The degree of these effects is estimated by the following equation

$$\Delta E = -\mathrm{sgn}(2p + 1)3t_0(1 + \nu)\sigma \cos 3\theta \quad (1)$$

Here p = mod(n − m, 3), t_0 (= 2.66 eV) denotes the hopping parameter, ν (= 0.2) represents the Poisson's ratio, and σ denotes the radial compression.[42] According to this equation, the calculated σ of the metallic NPDs is plotted as a function of tube diameter (red circles), together with that for the type II semiconducting NPDs (black circles) (Figure 5c). It is clearly seen that both metallic and semiconducting SWCNTs show similar diameter dependence of σ; however, the absolute values of σ for the metallic SWCNTs are slightly smaller than those for the semiconducting SWCNTs with similar diameters. These results are reasonably explained by the smaller interaction between metallic SWCNTs and the encapsulated C_{60}.

Even though theoretical calculations usually predict that aromatic molecules more strongly adsorb onto the surface of metallic SWCNTs than that of semiconducting SWCNTs,[43] a close similarity between the diameter dependence of $\Delta\omega$ (Figure 5a) and σ (Figure 5c) strongly suggests that the intermolecular interaction between metallic SWCNTs and the encapsulated C_{60} is weaker than that of semiconducting SWCNTs and C_{60}. This seems to be consistent with recent experimental results for metallic-semiconducting SWCNTs separations; aromatic polyfluorene was used to selectively extract semiconducting SWCNTs from a mixture of both metallic and semiconducting

SWCNTs[10,11,13] and extract fast eluent behaviors of metallic SWCNTs by the agarose gel method.[12] Although nearly 20 years have passed since the discovery of SWCNTs, many unknown aspects of their fundamental natures still need to be addressed.

CONCLUSIONS

In conclusion, the effects of C_{60} encapsulations on the RBM vibrational frequencies and the optical transition energies of metallic SWCNTs were systematically investigated by resonance Raman spectroscopy. The observed RBM frequency shifts and the changes in the optical transition energy can be reasonably explained by the intermolecular interaction, as in the case of semiconducting NPDs. However, the degree of the effects is smaller than that of semiconducting SWCNTs, thereby indicating modest interaction between metallic SWCNTs and the encapsulated C_{60}. The present findings provide important insights into the differences between the intrinsic natures of metallic and semiconducting SWCNTs.

ASSOCIATED CONTENT

Supporting Information

Curve-fitting analyses of the observed Raman spectra in RBM region. RBM frequencies (ω_{RBM}) and optical transition energies (E^{M}_{11}) of C_{60} NPDs and SWCNTs. This material is available free of charge via the Internet at http://pubs.acs.org.

AUTHOR INFORMATION

Corresponding Author

*E-mail: toshi.okazaki@aist.go.jp.

Author Contributions

The manuscript was written through contributions of all authors. All authors have given approval to the final version of the manuscript.

Notes

The authors declare no competing financial interest.

ACKNOWLEDGMENTS

We thank Mr. J. Kang (Sungkyunkwan University) for helping us in our experimental work. This work was partially supported by MEXT KAKENHI (#21685017).

REFERENCES

(1) Hamada, N.; Sawada, S.; Oshiyama, A. *Phys. Rev. Lett.* **1992**, *68*, 1579−1581.
(2) Saito, R.; Fujita, M.; Dresselhaus, G.; Dresselhaus, M. S. *Appl. Phys. Lett.* **1992**, *60*, 2204−2206.
(3) Deshpande, V. V.; Bockrath, M.; Glazman, L. I.; Yacoby, A. *Nature* **2010**, *464*, 209−216.
(4) Ishii, H.; Kataura, H.; Shiozawa, H.; Yoshioka, H.; Otsubo, H.; Takayama, Y.; Miyahara, T.; Suzuki, S.; Achiba, Y.; Nakatake, M.; Narimura, T.; Higashiguchi, M.; Shimada, K.; Namatame, H.; Taniguchi, M. *Nature* **2003**, *426*, 540−544.
(5) Deshpande, V. V.; Chandra, B.; Caldwell, R.; Novikov, D. S.; Hone, J.; Bockrath, M. *Science* **2009**, *323*, 106−110.
(6) Zhang, D.; Ryu, K.; Liu, X.; Polikarpov, E.; Ly, J.; Tompson, M. E.; Zhou, C. *Nano Lett.* **2006**, *6*, 1880−1886.
(7) Li, J.; Hu, L.; Wang, L.; Zhou, Y.; Grüner, G.; Marks, T. J. *Nano Lett.* **2006**, *6*, 2472−2477.
(8) Maeda, Y.; Kimura, S.; Kanda, M.; Hirashima, Y.; Hasegawa, T.; Wakahara, T.; Lian, Y. F.; Nakahodo, T.; Tsuchiya, T.; Akasaka, T.; Lu, J.; Shimizu, T.; Tokumoto, M.; Saito, R. *J. Am. Chem. Soc.* **2005**, *127*, 10287−10290.
(9) Arnold, M. S.; Green, A. A.; Hulvat, J. F.; Stupp, S. I.; Hersam, M. C. *Nat. Nanotechnol.* **2006**, *1*, 60−65.
(10) Nish, A.; Hwang, J.-Y.; Doig, J.; Nicholas, R. J. *Nat. Nanotechnol.* **2007**, *2*, 640−646.
(11) Chen, F.; Wang, B.; Chen, Y.; Li, L.-J. *Nano Lett.* **2007**, *7*, 3013−3017.
(12) Tanaka, T.; Jin, H.; Miyata, Y.; Kataura, H. *Appl. Phys. Exp.* **2008**, *1*, 11401.
(13) Tange, M; Okazaki, T.; Iijima, S. *J. Am. Chem. Soc.* **2011**, *133*, 11908−11911.
(14) Smith, B. W.; Monthioux, M.; Luzzi, D. E. *Nature* **1998**, *396*, 323−324.
(15) Monthioux, M. *Carbon* **2002**, *40*, 1809−1823.
(16) Guan, L.; Li, H.; Shi, Z.; You, L.; Gu, Z. *Solid State Commun.* **2005**, *133*, 333−336.
(17) Kaneko, T.; Li, Y.; Nishigaki, S.; Hatakeyama, R. *J. Am. Chem. Soc.* **2008**, *130*, 2714−2715.
(18) Caillier, Ch.; Machon, D.; San-Miguel, A.; Arenal, R; Montagnac, G.; Cardon, H.; Kalbac, M.; Zukalova, M.; Kavan, L. *Phys. Rev. B* **2008**, *77*, 125418.
(19) Yanagi, K.; Iakoubovskii, K.; Matsui, H.; Matsuzaki, H.; Okamoto, H.; Miyata, Y.; Maniwa, Y.; Kazaoui, S.; Minami, N.; Kataura, H. *J. Am. Chem. Soc.* **2007**, *129*, 4992−4997.
(20) Okazaki, T.; Iizumi, Y.; Okubo, S.; Kataura, H.; Liu, Z.; Suenaga, K.; Tahara, Y.; Yudasaka, M.; Okada, S.; Iijima, S. *Angew. Chem., Int. Ed.* **2011**, *50*, 4853−4857.
(21) Otani, M.; Okada, S.; Ohiyama, A. *Phys. Rev. B* **2003**, *68*, 125424.
(22) Chorro, M.; Delhey, A.; Noe, L.; Monthioux, M.; Launois, P. *Phys. Rev. B* **2007**, *75*, 035416.
(23) Verberck, B.; Michael, K. H. *Phys. Rev. B* **2007**, *75*, 045419.
(24) Okazaki, T.; Okubo, S.; Nakanishi, T.; Joung, S.-K.; Saito, T.; Otani, M.; Okada, S.; Bandow, S.; Iijima, S. *J. Am. Chem. Soc.* **2008**, *130*, 4122−4128.
(25) Okubo, S.; Okazaki, T.; Kishi, N.; Joung, S.-K.; Nakanishi, T.; Okada, S.; Iijima, S. *J. Phys. Chem. C* **2009**, *113*, 571−575.
(26) Joung, S.-K.; Okazaki, T.; Kishi, N.; Okada, S.; Bandow, S.; Iijima, S. *Phys. Rev. Lett.* **2009**, *103*, 027403.
(27) Joung, S.-K.; Okazaki, T.; Okada, S.; Iijima, S. *Phys. Chem. Chem. Phys.* **2010**, *12*, 8118−8122.
(28) Okubo, S.; Okazaki, T.; Hirose-Takai, K.; Suenaga, K.; Okada, S.; Bandow, S.; Iijima, S. *J. Am. Chem. Soc.* **2010**, *132*, 15252−15258.
(29) Iizumi, Y.; Okazaki, T.; Liu, Z.; Suenaga, K.; Nakanishi, T.; Iijima, S.; Rotas, G.; Tagmatarchis, N. *Chem. Commun.* **2010**, *46*, 1293−1295.
(30) Kataura, H.; Maniwa, Y.; Kodama, T.; Kikuchi, K.; Hirahara, K.; Suenaga, K.; Iijima, S.; Suzuki, S.; Achiba, Y.; Krätschmer, W. *Synth. Met.* **2001**, *121*, 1195−1196.
(31) Hornbaker, D. J.; Kahng, S.-J.; Misra, S.; Smith, B. W.; Johnson, A. T.; Mele, E. J.; Luzzi, D. E.; Yazdani, A. *Science* **2002**, *295*, 828−831.
(32) Shimada, T.; Okazaki, T.; Taniguchi, R.; Sugai, T.; Shinohara, H.; Suenaga, K.; Ohno, Y.; Mizuno, S.; Kishimoto, S.; Mizutani, T. *Appl. Phys. Lett.* **2002**, *81*, 4067−4069.
(33) Shiozawa, H.; Ishii, H.; Kihara, H.; Sasaki, N.; Nakamura, S.; Yoshida, T.; Takayama, Y.; Miyahara, T.; Suzuki, S.; Achiba, Y.; Kodama, T.; Higashiguchi, M.; Chi, X. Y.; Nakatake, M.; Shimada, K.; Namatame, H.; Taniguchi, M.; Kataura, H. *Phys. Rev. B* **2006**, *73*, 075406.
(34) Kavan, L.; Dunsch, L. *ChemPhysChem* **2007**, *8*, 974−998.
(35) Son, H.; Reina, A.; Samsonidze, Ge. G.; Saito, R.; Jorio, A.; Dresselhaus, M. S.; Kong, J. *Phys. Rev. B* **2006**, *74*, 073406.
(36) Araujo, P. T.; Jorio, A.; Dresselhaus, M. S.; Sato, K.; Saito, R. *Phys. Rev. Lett.* **2009**, *103*, 146802.
(37) Doorn, S. K.; Araujo, P. T.; Hata, K.; Jorio, A. *Phys. Rev. B* **2008**, *78*, 165408.
(38) Palser, H. A. R. *Phys. Chem. Chem. Phys.* **1999**, *1*, 4459−4464.
(39) Okada, S. *Chem. Phys. Lett.* **2007**, *438*, 59−62.
(40) Farhat, H.; Son, H.; Samsonidze, Ge. G.; Reich, S.; Dresselhaus, M. S.; Kong, J. *Phys. Rev. Lett.* **2007**, *99*, 145506.

(41) Farhat, H.; Sasaki, K.; Kalbac, M.; Hofmann, M.; Saito, R.; Dresselhaus, M. S.; Kong, J. *Phys. Rev. Lett.* **2009**, *102*, 126804.
(42) Yang, L.; Han, J. *Phys. Rev. Lett.* **2000**, *85*, 154−157.
(43) Lu, J.; Nagase, S.; Zhang, X.; Wang, D.; Ni, M.; Maeda, Y.; Wakahara, T.; Nakahodo, T.; Tsuchiya, T.; Akasaka, T.; Gao, Z.; Yu, D.; Ye, H.; Mei, W. N.; Zhou, Y. *J. Am. Chem. Soc.* **2006**, *128*, 5114−5118.